

### Diffraction analysis of pion elastic scattering from $^{40}\text{Ar}$

J.-F. Germond, E. Bovet, and J.-P. Egger  
*University of Neuchâtel, CH-2000 Neuchâtel, Switzerland*

G. S. Blanpied, C. S. Mishra, and B. M. Preedom  
*University of South Carolina, Columbia, South Carolina 29208*  
 (Received 13 May 1985)

Differential cross sections for pion elastic scattering from  $^{40}\text{Ar}$  at 180 MeV have been analyzed within the framework of diffraction theory. Using a phenomenological determination of the underlying pion dynamics, we deduce the ratios of  $^{40}\text{Ar}$  to  $^{40}\text{Ca}$  neutron and proton densities at a radius of 4.7 fm. The results obtained show that  $^{40}\text{Ar}$  has a neutron skin in excess of  $^{40}\text{Ca}$  and the reverse for the proton skin, in agreement with Hartree-Fock densities as well as previous determinations from  $\mu$  x rays and alpha scattering experiments.

It is well known that pion-nucleus elastic differential cross sections around the  $\Delta_{33}$  resonance exhibit an oscillatory pattern of geometrical character. Therefore, the appropriate variables to describe this type of experiments are those of diffraction theory, independent of the underlying microscopic theory. Such an approach was originally proposed by Johnson and Bethe<sup>1</sup> and further improved in Ref. 2. Application to the analysis of the pion data on the calcium isotopes was carried out in Ref. 3.

In this Brief Report we extend the analysis to  $\pi^+$  and  $\pi^-$  elastic data on  $^{40}\text{Ar}$  at 180 MeV obtained recently at SIN (Schweizerisches Institut für Nuklearforschung) with the  $\pi M1$  beam line and the SUSI spectrometer, details of which are given in Ref. 4. In order to take full advantage of the high incident pion flux ( $2 \times 10^7 \pi^+/\text{s}$  and  $4 \times 10^6 \pi^-/\text{s}$ ), the multiwire proportional chamber (MWPC) measuring the incident pion energy was replaced by a scintillator hodoscope. The target used was a 1.8-cm thick liquid argon vessel with two 0.2-mm thick stainless steel windows, cooled with liquid nitrogen. Target frame background was taken into account with empty target runs. The overall energy resolution was 2 MeV full width at half maximum (FWHM). The elastic peak was in general, sufficiently important to be well separated. However, at some angles the elastic peak shape was used to extract the cross section. For the same reasons (pion flux), the MWPC measuring the incident pion angle on target was replaced by a scintillator. This resulted in a worsening of the angular resolution which was corrected with a finite angular correction described, for example, in Ref. 5. The absolute normalization is correct within  $\pm 8\%$ . The angular distributions are presented in Fig. 1. A cross sections table can be obtained from J.-P.E.

The theoretical analysis of the present  $^{40}\text{Ar}$  data is based on the formalism and equations developed in Refs. 2 and 3 for the calcium isotopes. In these papers it was shown that the elastic scattering amplitude could be represented to a high degree of approximation by a very simple analytical form characterized by only three physically meaningful parameters  $b_1$ ,  $a$ , and  $Y$ . The quantity  $b_1$  determines the size of the diffractive disk, i.e., the position of the minima in the angular distribution,  $a$  the rate of falloff, and  $Y$  the relative real part of the scattering amplitude. The strong interaction amplitude is of the fuzzy black disk type,<sup>6</sup> whereas the Coulomb interaction gives rise to the usual Bethe phase<sup>7</sup> with trajectory distortion and energy shift effects included.<sup>8</sup>

The interested reader is referred to Ref. 2, for the exact formulas. The best fits to the present  $\pi^\pm$ - $^{40}\text{Ar}$  180-MeV data are shown on Fig. 1 and the corresponding values of the parameters quoted in Table I. Also quoted in Table I are the best-fit parameters obtained by analyzing our previous  $\pi^\pm$ - $^{40}\text{Ca}$  elastic scattering data<sup>9</sup> which will be used as reference in the extraction of the nuclear densities. Only data up

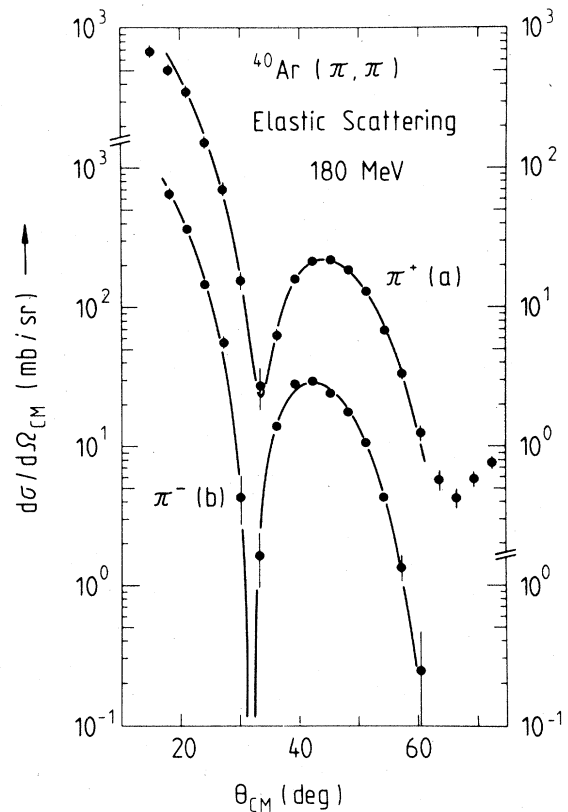


FIG. 1. Center of mass differential cross sections for  $\pi^+$  (a) and  $\pi^-$  (b) elastic scattering from  $^{40}\text{Ar}$  at 180 MeV. The data have been corrected for finite angular resolution. The curves are least squares fits to our analytical theory in the angular range  $18^\circ$ - $58^\circ$ . The corresponding values of the best-fit parameters  $b_1$ ,  $a$ , and  $Y$  are quoted in Table I.

TABLE I. Best-fit parameters for  $\pi^\pm$  elastic scattering from  $^{40}\text{Ar}$  and  $^{40}\text{Ca}$  at 180 MeV. Quoted errors are purely statistical.

Nucleus	$b_1$ (fm)	$a$ (fm)	$Y$
$^{40}\text{Ar}^a \pi^+$	$4.501 \pm 0.011$	$0.529 \pm 0.012$	$-0.142 \pm 0.053$
$\pi^-$	$4.717 \pm 0.015$	$0.507 \pm 0.016$	$-0.287 \pm 0.131$
$^{40}\text{Ca}^b \pi^+$	$4.588 \pm 0.007$	$0.606 \pm 0.008$	$-0.130 \pm 0.024$
$\pi^-$	$4.709 \pm 0.007$	$0.675 \pm 0.008$	$-0.122 \pm 0.028$

<sup>a</sup>This work.

<sup>b</sup>Data from Ref. 9.

to 58° were used in the fitting procedure since the analytical theory has been shown to reproduce accurately the magnitude of the cross sections only up to the first subsidiary maximum.<sup>2</sup> The parameters  $b_1$ ,  $a$ , and  $Y$  of Table I carry the essential features of data and will now be used to extract information on the nuclear densities. In order to achieve this goal we compare these values to those of a neighboring nucleus, namely,  $^{40}\text{Ca}$  by computing first the auxiliary quantities

$$\beta = \left( \frac{a_0^{\text{Ca}} \tilde{b}_1^{\text{Ca}}}{a_0^{\text{Ar}} \tilde{b}_1^{\text{Ar}}} \right)^{1/2} \frac{e^{(\tilde{b}_1 - \tilde{b}_1^{\text{Ca}})/a_0^{\text{Ca}}}}{e^{(\tilde{b}_1 - \tilde{b}_1^{\text{Ar}})/a_0^{\text{Ar}}}}, \quad (1)$$

which can be entirely determined from the parameters of Table I with the choice  $\tilde{b}_1 = 4.7$  fm. The  $\tilde{b}_1$ 's in Eq. (1) are actually the Coulomb corrected values of  $b_1$  evaluated according to

$$\tilde{b}_1 = b_1 + \frac{\eta}{k}, \quad (2)$$

where  $\eta$  is the Sommerfeld parameter and  $k$  the pion wave number. Since we evaluate  $\beta$  for  $\pi^+$  and  $\pi^-$  separately and since the  $^{40}\text{Ar}$  charge differs by only 10% from that of  $^{40}\text{Ca}$ , all other residual Coulomb corrections can be safely ignored. Furthermore, the quantities  $a_0$  in Eq. (1) are related to  $a$  by

$$a_0 = a(1 + a/2\tilde{b}_1)^{-1}, \quad (3)$$

and correspond to the distance over which the nuclear density falls by  $1/e$  of its value at  $\tilde{b}_1$ . The deduced values for  $\beta$  are

$$\beta_+ = 0.88 \pm 0.02, \quad \text{for } \pi^+, \quad (4a)$$

$$\beta_- = 1.13 \pm 0.04, \quad \text{for } \pi^-. \quad (4b)$$

On the other hand, these quantities  $\beta$  are equal to the ratio of the  $^{40}\text{Ar}$  to the  $^{40}\text{Ca}$  pion optical potential evaluated at the common point  $\tilde{b}_1$ . This allows us to obtain the  $^{40}\text{Ar}$  proton and neutron densities relative to the  $^{40}\text{Ca}$  densities at  $r = \tilde{b}_1$ ,

$$\rho_p^{\text{Ar}}/\rho_p^{\text{Ca}} = \frac{1}{2\gamma} [\beta_+ (1 + \frac{1}{2}\gamma)^2 - \beta_- (1 - \frac{1}{2}\gamma)^2 - (1 - \gamma^2/4)(\beta_- - \beta_+) \rho_n^{\text{Ca}}/\rho_p^{\text{Ca}}], \quad (5a)$$

$$\rho_n^{\text{Ar}}/\rho_n^{\text{Ca}} = \frac{1}{2\gamma} [\beta_- (1 + \frac{1}{2}\gamma)^2 - \beta_+ (1 - \frac{1}{2}\gamma)^2 + (1 - \gamma^2/4)(\beta_- - \beta_+) \rho_p^{\text{Ca}}/\rho_n^{\text{Ca}}], \quad (5b)$$

where the parameter  $\gamma$  denotes the ratio of isovector to isoscalar optical potential relative to its value obtained from the free pion-nucleon scattering amplitude. In particular,  $\gamma = 1$  corresponds to the usual first order optical potential but phenomenological analysis of single charge exchange experiments on a wide variety of nuclei<sup>10</sup> have required a value of  $\gamma$  larger than unity. The necessary increase of the isovector part of the optical potential is presumably coming from dynamical and medium effects arising at the level of second order in density.<sup>11</sup> In this paper we shall adopt the value  $\gamma = 1.3$  deduced from the analysis of the pion elastic scattering data on the calcium isotopes.<sup>3</sup> The ratio  $\rho_n^{\text{Ca}}/\rho_p^{\text{Ca}}$  ( $r = 4.7$  fm) appearing in Eqs. (5) will be fixed equal to its value 0.941 predicted by Hartree-Fock calculations.<sup>12</sup> The results for the  $^{40}\text{Ar}$  proton and neutron densities relative to  $^{40}\text{Ca}$  can be found on the first two lines of Table II. They are in good agreement with the predictions of Hartree-Fock BCS calculations also shown in Table II. By comparing to nuclear densities scaled by the number of protons or neutrons we see that  $^{40}\text{Ar}$  has a neutron halo compared to  $^{40}\text{Ca}$  and the reverse for the proton density. This can be seen more clearly in the last two lines of Table II, where differences of root mean square (rms) radii are quoted. In order to calculate radii from pion elastic scattering data we *must* rely on a model for the shape of the densities. We stress that pion elastic scattering at resonance is sensitive to the tail of the nuclear densities and not to the rms radii. The values of rms radii quoted in Table II have been obtained by using a Woods-Saxon shape whose average parameters were fixed to the calcium nuclear densities. Our deduced value for the shift of the proton rms radius between  $^{40}\text{Ca}$  and  $^{40}\text{Ar}$  agrees with determinations from  $\mu$  x-rays experiments<sup>13</sup> and the same is true for the neutron rms radius

TABLE II. Ratio of proton (neutron) densities  $\rho_p$  ( $\rho_n$ ) at  $r = 4.7$  fm and shift of rms radii  $r_p$  ( $r_n$ ) between  $^{40}\text{Ar}$  and  $^{40}\text{Ca}$  compared to Hartree-Fock calculations,  $\mu$  x-rays and alpha scattering experiments.

	$\pi$ -nucleus <sup>a</sup>	Hartree-Fock <sup>b</sup>	$\mu$ x-rays <sup>c</sup>	$\alpha$ -nucleus <sup>d</sup>
$\rho_p^{\text{Ar}}/\rho_p^{\text{Ca}}(r = 4.7 \text{ fm})$	$0.82 \pm 0.03$	0.81		
$\rho_n^{\text{Ar}}/\rho_n^{\text{Ca}}(r = 4.7 \text{ fm})$	$1.20 \pm 0.05$	1.21		
$r_p^{\text{Ar}} - r_p^{\text{Ca}} \text{ (fm)}$	$-0.06 \pm 0.02^e$	-0.08	$-0.057 \pm 0.008$	
$r_n^{\text{Ar}} - r_n^{\text{Ca}} \text{ (fm)}$	$0.05 \pm 0.03^e$	0.08		$0.11 \pm 0.09$

<sup>a</sup>This work, statistical errors only.

<sup>b</sup>Reference 12.

<sup>c</sup>Reference 13.

<sup>d</sup>Reference 14.

<sup>e</sup>Values deduced by assuming a Woods-Saxon shape for the nuclear densities.

shift compared to the one obtained from alpha particle scattering data.<sup>14</sup> However, statistical error bars are still very large. Although they could be reduced by increasing the data taking time and the angular resolution we then would be confronted with systematic uncertainties in the theory such as residual Coulomb effects, dependence of  $\gamma$  on nuclear densities, nonlocal effects, and noneikonal corrections.

In conclusion, we have shown that our simple analysis of pion elastic scattering data on  $^{40}\text{Ar}$  at 180 Mev is able to provide valuable information about the proton and neutron densities. The same semiclassical analysis can be used to calculate pion single charge exchange amplitudes to isobaric

analog states (IAS). Using the deduced values of Table II we predict for  $^{40}\text{Ar}$  ( $\pi^+$ ,  $\pi^0$ ) $^{40}\text{K}$ (IAS) a  $0^\circ$  differential cross section of approximately 0.9 mb/sr. A measurement of this reaction would further confirm the values obtained in Table II for the  $^{40}\text{Ar}$  proton and neutron densities.

We are very grateful to R. Lombard for providing us with the Hartree-Fock densities calculations and for useful discussions. We also thank M. B. Johnson for correspondence. This work was partially supported by the Swiss National Science Foundation and by the U.S. National Science Foundation.

<sup>1</sup>M. B. Johnson and H. A. Bethe, *Comments Nucl. Part. Phys.* **8**, 77 (1978).

<sup>2</sup>J.-F. Germond and M. B. Johnson, *Phys. Rev. C* **22**, 1622 (1980).

<sup>3</sup>J.-F. Germond, M. B. Johnson, and J. Johnstone, *Phys. Rev. C* (to be published).

<sup>4</sup>J. P. Albanèse *et al.*, *Nucl. Instrum. Methods* **158**, 363 (1979).

<sup>5</sup>F. Binon *et al.*, *Nucl. Phys. B* **17**, 168 (1970).

<sup>6</sup>E. V. Inopin and Y. A. Berezhnoy, *Nucl. Phys.* **63**, 689 (1965).

<sup>7</sup>H. A. Bethe, *Ann. Phys. (N.Y.)* **3**, 190 (1958).

<sup>8</sup>J.-F. Germond and C. Wilkin, *Ann. Phys. (N.Y.)* **121**, 285 (1979).

<sup>9</sup>P. Gretilat *et al.*, *Nucl. Phys.* **A364**, 270 (1981).

<sup>10</sup>S. J. Greene *et al.*, *Phys. Rev. C* **30**, 2003 (1984).

<sup>11</sup>M. B. Johnson and E. R. Siciliano, *Phys. Rev. C* **27**, 730 (1983);

**27**, 1647 (1983).

<sup>12</sup>R. J. Lombard (private communication); see also M. Beiner and R. J. Lombard, *Ann. Phys. (N.Y.)* **86**, 262 (1974).

<sup>13</sup>H. Daniel *et al.*, *Phys. Lett.* **48B**, 109 (1974); H. D. Wohlfahrt *et al.*, *ibid.* **73B**, 131 (1978); H. D. Wohlfahrt, in *Proceedings of the Karlsruhe International Discussion Meeting, Karlsruhe, 1979*, edited by H. Rebel, H. J. Gils, and G. Schatz (Kernforschungszentrum Karlsruhe, Karlsruhe, 1979), p. 57.

<sup>14</sup>F. Michel, in *Proceedings of the Karlsruhe International Discussion Meeting, Karlsruhe, 1979*, edited by H. Rebel, H. J. Gils, and G. Schatz (Kernforschungszentrum Karlsruhe, Karlsruhe, 1979), p. 200; *Phys. Lett.* **82B**, 183 (1979).